Characterization of Mo-Re/ZSM-5 Catalysts: How the Rhenium Improves the Performance of Mo in the Methane Dehydroaromatization Reaction

A. López-Martín[a], F. Sini[b], M.G. Cutrufello[b], A. Caballero[a†] and G. Colón[a†]

[a] *Instituto de Ciencia de Materiales de Sevilla. Centro Mixto Universidad de Sevilla-CSIC. Américo Vespucio s/n. 41092 Sevilla. Spain*

[b] *Dipartimento di Scienze Chimiche e Geologiche. Università di Cagliari. Complesso Univ Monserrato, SS 554 Bivio Sestu. 09124 Cagliari, Italy*

[†] corresponding authors: caballero@us.es and gcolon@icmse.csic.es

Abstract

In this study, the promoting effect of rhenium addition as a co-dopant on Mo/ZSM-5 catalysts system has been analysed. Hence, bimetallic (Re-Mo/ZSM-5) catalysts have been synthesized using a sequential impregnation methodology. The catalytic performance for direct aromatization of methane reaction has been determined and correlated with their physical and chemical state, combining chemical (TPR), spectroscopic (XPS), electron microscopy (TEM, HAADF) and other characterization techniques. An important synergy between Mo and Re, which it is affected by the sequential impregnation, has been observed. Thus, Re1-Mo4/ZSM-5 in which rhenium has been incorporated first shows notably higher aromatic yields as well as higher stability against deactivation with respect to former monometallic systems. The characterization results suggest that this catalytic enhancement is due to the important effect of Re presence in close interaction with Mo. Improved evolution of ethane through C-C coupling would be correlated to this catalytic performance. As we discussed, Mo nature and location in the bimetallic systems are strongly conditioned by Re and the impregnation sequence and would favour such intermediate step.

Keywords: bimetallic, molybdenum, rhenium, methane dehydroaromatizacion.

Introduction

Non-oxidative catalytic methane dehydroaromatization (*MDA*) to benzene provides a potential route for direct production of benzene from methane resources. *MDA* was first reported more than 25 years ago by Wang *et al*. [1], and the increasing availability of cheap natural gas has attracted growing interest at this direct route for the conversion of methane into high-value chemicals [2]. Several research works have been published on this topic in the last few decades. However Mo/HZSM-5, found by Wang in 1993, is still the preferred catalyst for *MDA* reaction [3]. Challenges with the MDA reaction are two-fold: the reaction is thermodynamically limited with low one-pass methane conversion and even the best catalytic systems, Mo/zeolites, suffer rapid deactivation from coking [4]. Within this framework, several characteristics are yet unknown and how to prevent its deactivation caused by coke formation still remains an unsolved problem that hinders its industrial application [5,6,7].

In order to improve the catalytic performance and to decrease the deactivation rate, multiple studies have studied the addition of different metals as a co-dopants to the Mo catalysts. However, though reported results showed interesting effects, attained improvements appears always temporary and the stability of the catalysts was always a challenge [8]. For this sake, a catalyst design strategy is crucial to improve stability. So, the use of multifunctional Mo-X/zeolite systems where X is a co-dopant capable of modulating the stability has been widely reported. In this sense, the addition of metal dopants to would improve not only the catalytic performance but also the stability of Mo/ZSM-5 catalysts by influencing the catalyst deactivation step.

Thus, Scurrell and co-workers added platinum and/or tin on Mo/ZSM-5 zeolite catalyst for methane aromatization reaction [9]. They concluded that catalysts with additional tin led to lower methane conversion but higher aromatic products selectivity. Abdelsayed *et al* introduced Fe

and/or Zn to modify conventional Mo/ZSM-5 catalysts, demonstrating that Fe−Mo/ZSM-5 displayed high stability and selectivity to aromatics [10]. Zhang *et al* studied the effect of indium on Mo/ZSM-5 in *MDA* concluding that although methane conversion decreases, the coke selectivity is reduced to 50% that of Mo/ZSM-5 [11]. Such stabilization seems to be related to the close proximity of In and Mo that would suppress coke formation. More recently, Sridhar *et al* reported the addition of different loadings of Co and Ni on Mo/ZSM-5 catalyst in order to evaluate the promoting effect of these metals on reactivity and stability of the Mo catalysts [12]. They observed a synergistic effect between Mo and the promoters, resulting in benzene yield and catalytic stability improvements.

Since it is proposed that Brönsted acid sites would play an important role in the reaction pathways, the modification of the zeolite acidity would be achieved through metal co-doping [13]. Thus, Cr, Ag and Ga were employed as additive that increased the catalyst acidity and resulted in improved methane conversion and benzene selectivity [8].

In this paper we study the effect of rhenium addition as co-dopant to the classical Mo/ZSM-5 catalyst, and how it affects, on the one hand to the physicochemical properties, and on the other hand to the catalytic activity and stability during *MDA* reaction. We will study the important effect of the sequential addition of metals, preparing two different series of catalyst in which Mo has been loaded first in a case (Mo1st), and Re in the other (Re1st). Both catalyst series have been widely characterized by several techniques, in particular XPS and TPR, and also tested in order to evaluate its catalytic performance in the *MDA* reaction.

Experimental Section

Catalyst preparation.

The bimetallic catalysts were prepared using a commercial NH_4-ZSM-5 zeolite (Alfa Aesar, Si/Al=23/1) previously calcined at 550 ºC for 3 hours to obtain the acid form. Mo and Re were sequentially added by impregnation procedure. Thus for each series, one of the metal was firstly impregnated followed by calcination at 550 ºC, 3h. After which, the second metal was subsequently introduced and further calcined again at the same temperature. The obtained series were named as Mo1st and Re1st.

Molybdenum was loaded using ammonium heptamolybdate tetrahydrate of appropriate concentration ($(NH_4)_6Mo_7O_{24}\cdot 4H_2O$, Sigma Aldrich) to obtain 4 wt%. Mo, while rhenium was loaded using rhenium (VII) oxide (Re_2O_7, Sigma Aldrich) at the corresponding stoichiometric amount leading to 1 wt% and 4 wt%. As a result, the following bimetallic systems were obtained: Re1-Mo4 and Re4-Mo4.

Catalytic activity in the Methane Dehydroaromatization (MDA).

The experimental measurements were accomplished with 0.1 g of catalyst diluted in 0.1 g of SiC, using a stainless-steel tubular reactor equipped with a temperature controller and four mass flow controllers. The stainless-steel reactor without catalyst, charged just with 0.2 g of SiC, was completely inactive for the *MDA* reaction. The catalyst was typically heated at 700 ºC for 18 h at atmospheric pressure. Methane dehydroaromatization reaction was performed under CH_4 /N_2 (85 %) flow (5 mL/min), from 50 ºC to 700 °C with a 10 °C/min temperature ramp. Reactants and reaction products were monitored by means of a previously calibrated GC 7890B. All lines connecting the reactor and GC were heated in order to avoid condensation of products.

Conversion and selectivity values were calculated according to the following mathematical expressions:

$Conversion(\%) = \frac{[CH_4]_t}{[CH_4]_i} \times 100$,

where $[CH_4]_t$ represent the moles of reacted methane and $[CH_4]_i$ the initial methane amount.

$Selectivity\ to\ product\ i(\%) = \frac{[product_i]_t \times n_i}{\sum [product_i]_t \times n_i} \times 100$,

where $[product_i]_t$ represents the moles of the specific product, n_i the number of C atoms in the product molecule (6 for benzene) and $\sum [product]_i$ the sum of moles from all products in the reaction. The aromatic selectivity has been determined as the sum of benzene, naphthalene and toluene.

Characterization techniques.

BET surface area measurements were carried out by N_2 adsorption at -196 ºC using a Micromeritics Tristar II instrument.

X-ray powder diffraction patterns of the studied catalysts were obtained by using a Siemens D-501 diffractometer with Ni filter and graphite monochromator and using the Cu K_α radiation.

TPR analysis were carried out using a Quantachrome Chemstar instrument equipped with a thermal conductivity detector and a mass spectrometer. About 40 mg of catalyst was first heated to 150 °C in an inert flow of Ar at 30 mL/min for 60 min previous to each experiment. The experimental conditions were chosen to fulfil the resolution conditions, according to the indication included in a previous work [14,15].

Ammonia adsorption microcalorimetry measurements were performed with a Tian-Calvet heat flow microcalorimeter (Setaram), equipped with a volumetric vacuum line. Each sample (ca. 0.1

g, 40-80 mesh) was thermally pretreated at 80 °C for 12 h under vacuum (5 mPa). Ammonia adsorption was carried out by admitting successive doses of the probe gas and measuring the equilibrium pressure relative to each adsorbed amount by means of a differential pressure gauge (Datameritics) up to a final equilibrium pressure of about 133 Pa. The thermal effect corresponding to the adsorption of each dose was simultaneously recorded. The adsorption temperature was kept at 80 °C, in order to limit physisorption. After overnight outgassing at the same temperature, a readsorption run was carried out, in order to distinguish the acid sites weak enough to be made free through the outgassing step. The adsorption and calorimetric isotherms were obtained from each adsorption (and readsorption) experiment. Combining the two sets of data, a plot of the differential heat of adsorption, Q_{diff}, as a function of the adsorbed amount was drawn, which gives information on the strength distribution of the adsorbing sites.

XPS data were recorded on pellets which were outgassed in the prechamber of the instrument at room temperature up to a pressure below $2 \cdot 10^{-8}$ torr to remove chemisorbed water. Thermal treatments were accomplished in a cell directly attached to the main chamber, allowing treatment while in contact with a mixture of gases emulating the TPR experiments. Spectra were recorded using a VG Scalab 210 spectrometer, working with constant pass energy of 50 eV. The spectrometer main chamber, working at a pressure below $2 \cdot 10^{-9}$ torr, is equipped with a Specs Phoibos 100 hemispherical electron analyser with a dual X-ray source working with Mg Kα (hν= 1254 eV) at 120 W and 30 mA. Si *2p* signal (103.0 eV) was used as the internal energy reference in all the experiments.

The transmission electron microscopic (TEM) images, high angle annular dark field (HAADF) and element mapping analysis images were obtained on the equipment FEI S/TEM Talos F200S. Samples were prepared by dipping a carbon grid in to the powder sample.

Results and Discussion

Methane dehydroaromatization (MDA)

The first important issue to point out is that Re incorporation significantly improves the benzene/aromatic yield in both series with respect to Mo monometallic system. Moreover, it is worthy to note that the catalytic activity for methane aromatization to benzene reveals that the addition sequence followed would have a marked effect. Thus, Re1st series shows better catalytic performance with respect to Mo1st one. The maximum activity is attained by Re1-Mo4/ZSM-5 catalyst in the Re1st series, for which higher production of benzene and aromatics has been found (**Figure 1)**. It is also worth of noting that the increasing amount of Re does not affect to the yield of benzene in the Re1st series. On the contrary, for Mo1st series increasing amount of Re seem to be detrimental. Moreover, in the case of aromatics production, irrespective of the sequence addition, higher Re content leads to a slightly lower yield. Thus, from both results it can be argued that Re1-Mo4/ZSM-5 from Re1st series would favor the naphthalene production with respect the other systems.

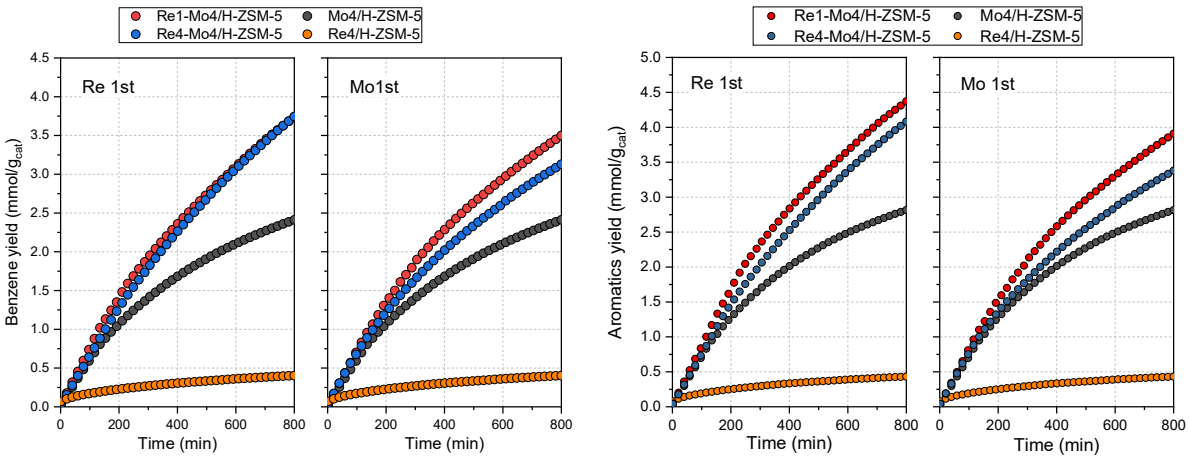

Figure 1. Benzene and aromatics yields for Mo4/ZSM-5, Re4/ZSM-5 and bimetallic catalysts for Mo1st and Re1st series.

Specifically, after 800 min in stream the obtained aromatics yield was 4.4 mmol/g_{cat} for the Re1-Mo4/ZSM-5 within Re1st series, being significantly higher than the observed value using Mo4/ZSM-5 sample, for which 2.5 mmol/g_{cat} is obtained.

Another interesting aspect concerns the evolution of intermediates. Early proposed mechanism argued that methane would react on the Mo sites to produce ethylene, which further proceeds on the acid sites of the two catalysts to form aromatics (both benzene and coke precursors). In a first step, ethane could be formed from methane coupling reaction [16]. Then, in a second step, ethane would undergo dehydrogenation to ethylene.

However, a recent report questioned the bifunctional mechanism in which ethylene would be the primary intermediate [15]. Vollmer et al proposed that ethylene would not be the major reaction intermediate since the hydrocarbon pool formed in the zeolite matrix during MDA is comprised of less dense and more hydrogenated species than the pool formed from ethylene. The hydrocarbon pool would be formed during the kinetic induction period and consist on compounds trapped within the voids.

If we observe the production of these intermediates for both series (Figure 2), it is clear that while ethylene formation is not affected by the presence of Re nor the preparation sequence, in the case of ethane important differences can be observed. Such different evolution would point out the fact that ethylene is not the primary but a side intermediate formed. Indeed, in a recent kinetic study Razdan et al, proposed that ethane is the initial product of C–C coupling [17]. The occurrence of Re and particularly when incorporated first, would be directly associated to the enhanced ethane evolution. Thus, it can be assumed that the differences in the aromatics production could be consequently associated in part to the best performance in C-C coupling step to ethane.

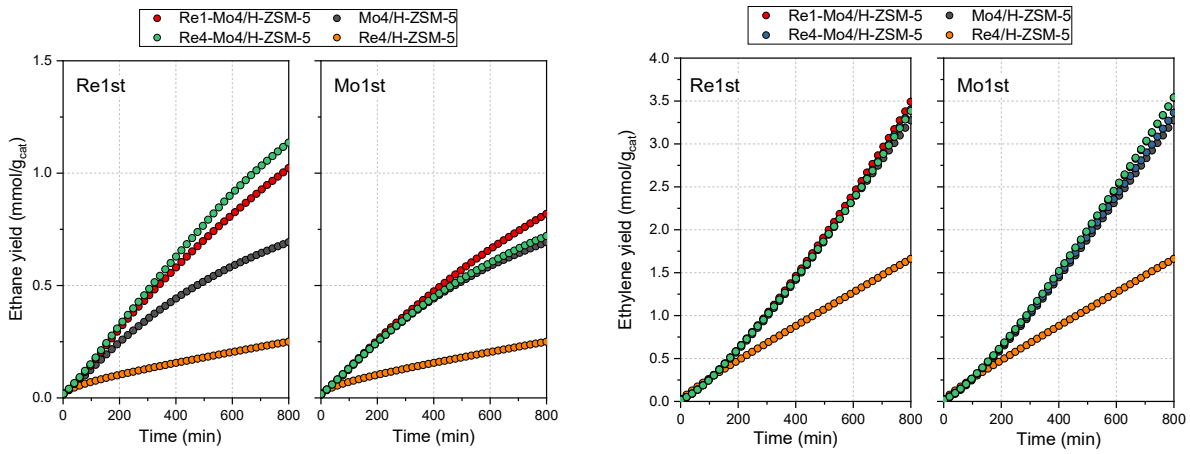

Figure 2. Evolution of ethane and ethylene formed during aromatization reaction over different catalysts from both series.

Characterization of calcined and reduced catalysts

In order to delve into the origin of the observed differences in the catalytic behaviour of the Re-Mo bimetallic catalysts, the systems were widely structural, textural and electronic characterized. As showed in **Figure 3**, the introduction of metal in the zeolite certainly affects to surface features of the catalyst. Thus, a slight decrease in the BET surface is observed for Mo and Re monometallic catalysts and occurs in both the micropores and mesopores surfaces in a similar way. Such decrease is largest in the case of Re4 monometallic system, where BET change from 360 m^2/g for the ZSM-5 to 231 m^2/g for Re4/ZSM-5. This diminution in the BET value is significantly lower than that exhibited by Mo4 sample. From this result it can be inferred that Re would percolate better than Mo inside the porous structure during calcination causing the pore blockage, particularly

micropore ones [7,18]. This effect has been previously reported for Re-MFI system [19]. In this study, Lacheen *et al* stated that through thermal treatment of Re_2O_7/H−MFI mixtures, the selective grafting of isolated and stable Re-oxo species via Re_2O_7 (g) reactions with OH groups to form $Si{-}O_fReO_3{-}Al$ is achieved. Moreover, grafting onto exchange sites would prevent the ubiquitous sublimation of ReO_x species.

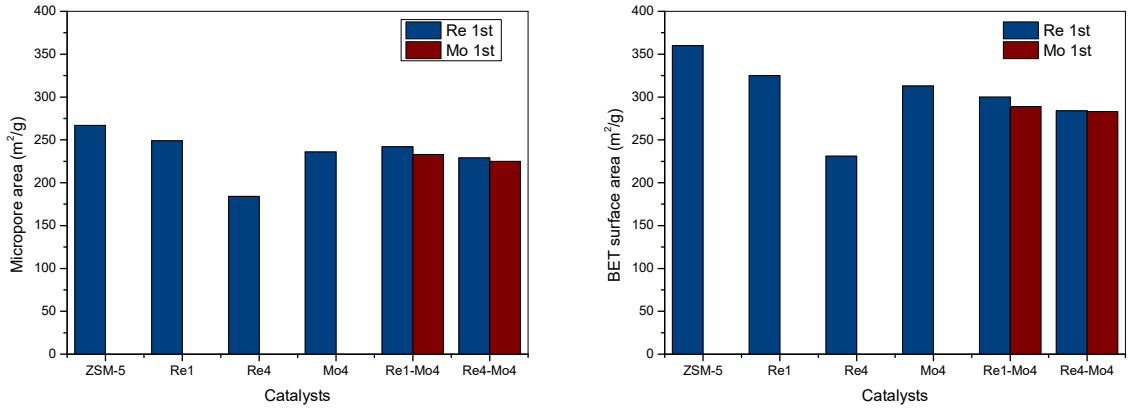

Figure 3. BET and micropore area results for the different catalysts prepared by both sequential methods.

It is surprising that bimetallic systems show similar surface features than monometallic Mo4/ZSM-5. Therefore, it appears that the changes in the surface area values are not related with the total metal loading. Moreover, the particular pore obstruction observed for monometallic Re seems not be present in these bimetallic samples. The surface area of Re4/ZSM-5 is smaller than Re4-Mo4 catalyst for which the metal loading is nearly double. Only a gradual decrease in the surface area with the total metal load increase is observed.

Comparing the Re-Mo systems between both series, it can be noticed that the introduction of Mo first (Mo1st series) led to a slightly lower surface area values than when Re is firstly impregnated

(Re1st series). As a consequence of the observed evolution, we would may infer that initial drastic pore obstruction by Re ions is not taking place in Re1st series. Indeed, for these samples, once Re is impregnated the solid is submitted to a further calcination process upon Mo incorporation. If we consider the high mobility of Re at moderate temperatures, it can be assumed that ions located at the inner micropore sites could be extracted and occupied the external surface or even partially sublimated. On the other side, when Re is incorporated in second place, it could be preferentially deposited close to Mo in close interaction as will be further discussed. This could explain that bimetallic samples do not show important diminution in the surface area. In spite of the different impregnation procedure, we have evidenced from HADDF a good dispersion of Re ions on the zeolite support (**Figure S1**). This fact denotes that Re would easily diffuse through zeolite pore structure upon different calcination treatments.

Ammonia adsorption microcalorimetry experiments were carried out to determine the total number, strength and strength distribution of surface acid sites. The differential heats of ammonia adsorption at 80 ºC on selected catalysts are presented in **Figure 4.a** with increasing surface coverage. The populations of the surface acid sites at various heat intervals of adsorption are shown in **Figure 4.b**. For all samples, after outgassing at 80 °C, NH_3 readsorption occurred only to a limited extent and with low values of differential heat of adsorption (Q_{diff} from 100 kJ/mol down to 60 kJ/mol). This indicates that the sites characterized by $Q_{diff} \leq 100$ kJ/mol are weak enough to readily desorb ammonia molecules adsorbed during the first adsorption run. Therefore, they can be classified as weak. By observing the different distribution of sites for weak, medium and strong acid sites it can noted that the incorporation of metals largely affects the weak acid sites. Moreover, it can be pointed out that Mo incorporation only affects these weak sites (60-100

kJ/mol). When Re is present, it is worthy to note that strongest sites (> 100 kJ/mol) are specifically affected.

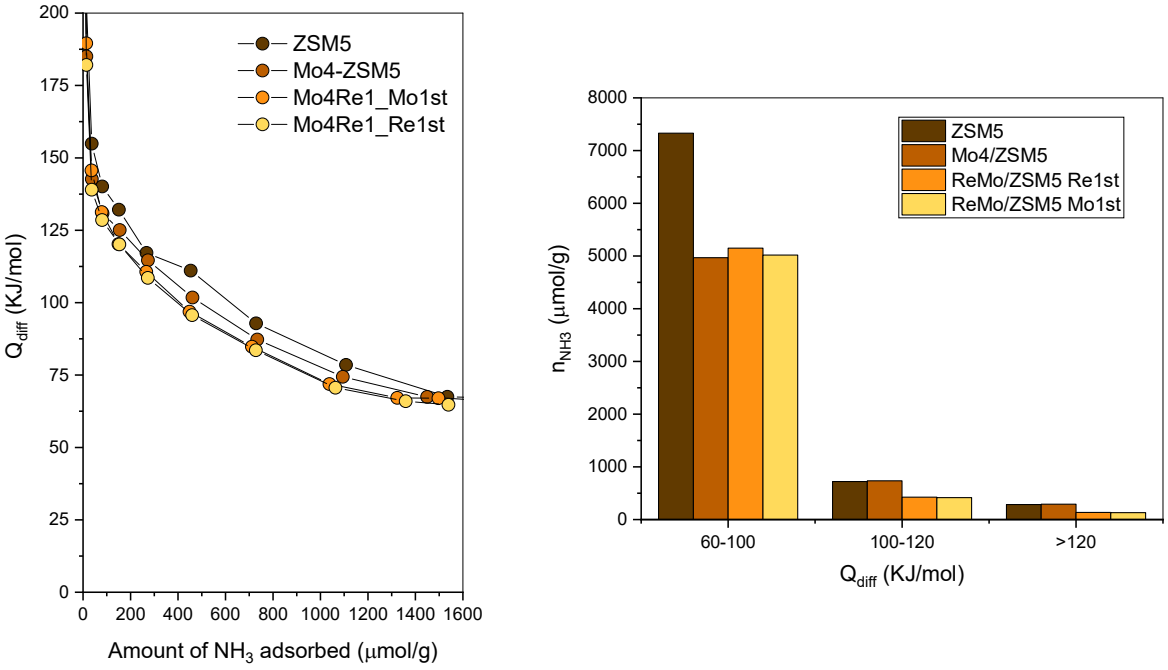

Figure 4. a) Differential heats of ammonia adsorption and b) Acid sites strength distribution obtained after ammonia adsorption for different catalysts.

In addition, it can be said that the sequence of metal incorporation in bimetallic systems would not have a clear effect on the number of these stronger acid sites. From these results, it can be argued that Re naturally trends to occupy the strongest sites while Mo the weakest ones. Such differential behavior could be related with the different acid character of the Mo and Re ions. In a recent work, Gao *et al* described that the strong interaction between acidic proton and Mo sites correlates with the products formation and catalyst lifetime [20]. These authors argued that this issue would have an important implication in modulating the catalytic MDA performance by taking advantage of

the proximity of the acidic proton-Mo sites at atomic-level. Furthermore, Wang *et al* argued that tuning the surface acidity of charged catalyst would balance the aromatization performance and coke resistance for stability enhancement [21]. Thus, as they reported, the strong Lewis and Brönsted acidity of Ag/ZSM-5 would be closely related to its good catalytic performance towards aromatization.

Thus, in our case, as stated from microcalorimetry, such stronger acid sites would be occupied by Re ions that would condition Mo location and therefore favour the interaction with these acid sites. This fact would be associated to the particular ethane evolution observed (**Figure 2**).

Figure 5 depicts the TPR profiles obtained for the samples. As we have shown in previous works [22,23], Mo4/ZSM-5 sample showed a complex TPR profile. Thus, we proposed the occurrence of different molybdenum oxides species, that changed as the metal loading increases. Essentially we reported four main reduction processes for this monometallic Mo sample (whose reducing processes peaked are at 510 ºC, 615 ºC, 755 ºC and 1000 ºC), showing the high heterogeneity of the chemical states of molybdenum supported on zeolite. On the other hand, Re reduction is much simpler and only one defined reduction peak is observed at ca. 400 ºC (**Figure S2**).

In the case of bimetallic catalysts, the reduction profile is quite different from monometallic references and cannot be represented as the sum of both profiles. This fact would point out that certain Mo-Re interaction is present. Such assumption would also be in agreement with the particular evolution of surface feature discussed above (**Figure 3**). Moreover, particularly for Re1-Mo4 systems, it appears that metal introduction sequence also affects to the reduction profile. Thus, this catalyst from Re1st series (**Figure 5**), the sharp peak associated to Re reduction appears shifted to a slightly higher temperature with lower intensity and showing a new notable shoulder. At the same time, most of the reduction peaks associated to Mo appeared in certain extent

diminished. This change in the TPR profile would imply a different reorganization of Mo ions in the structure with respect to the monometallic system. As we have previously stated [22], the highest reduction temperature (ca 1000 ºC) has been associated to Mo species located at the inner zeolite pores. Therefore, the diminution of this particular reduction peak would be associated to the presence of Re ion that could avoid the insertion of Mo at this inner sites. Moreover, the new important reduction process at ca 450 ºC together with the partial disappearance of Mo reduction peaks would indicate that Mo is reduced at lower temperatures in the presence of Re. It is worthy to mention that Re1-Mo4/ZSM-5 sample from Re1st series showed a more marked different profile with respect to monometallic Mo4/ZSM-5. We could infer that main diminution in the TPR profile is attained in the region 800º - 920 ºC (**Figure 5**). If we consider the different species described in a previous work, this reduction temperature range would be associated to external located bulk MoO_3. From HAADF images we unequivocally showed that these species would be supported on aluminium oxide segregated from the zeolite network and would be responsible of the heavy coke formation [22]. The particular modifications observed in this sample were not so marked for the same catalyst in the Mo1st series (**Figure 5**); so the different sequential deposition clearly induces a different structural situation. For this series, it seems that the TPR peak that appeared more affected was that at higher temperature. Thus, reduction peak has been associated to the well dispersed Mo-monomers located at the inner micropores with strong interaction with the support. The diminution of this reduction peak in this series would point out that upon Re incorporation these Mo species would diffuse to other positions, becoming easily reducible.

In the case of Re4-Mo4 catalysts, the TPR profiles do not show important differences between both series. It is worthy to note that in spite of the higher Re loading with respect to Re1-Mo4 catalysts the low temperature peak in principle associated to Re reduction appears with similar

intensity as in the case of Re1-Mo4 catalysts. This fact would denote that the reduction would not be complete.

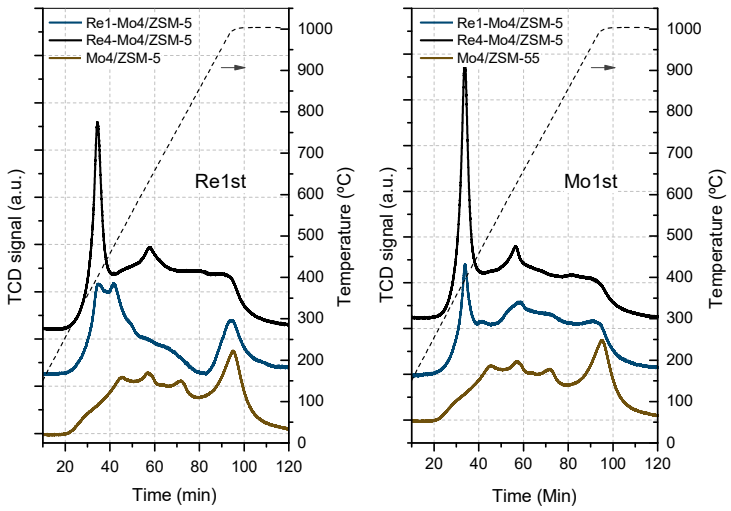

Figure 5. TPR profiles of monometallic Mo4/ZSM-5, and bimetallic Re-Mo/ZSM-5 catalysts from both series.

If we consider the metal content for both series (**Table 1**), it is worthy to note that while Mo content appears in all cases close to the nominal one, in the case of Re it can be noticed that for Re1st series the metal content is lower. This fact could be related with the high mobility of Re previously mentioned. Indeed, it has been reported that Re_2O_7 sublimation would occur at 250 ºC [24]. This fact has been used for achieving stable Re-oxo species grafted on zeolite precursors via Re_2O_7 (g) reactions with OH groups [19]. That issue has been pointed out from surface acidity discussion.

Indeed, for Re1st series the second calcination after Mo impregnation would provoke certain metal sublimation that lead to the slight metal loading diminution. Moreover, this process would explain that inner micropores that initially were blocked became free after the second calcination due to the migration toward the external surface. Such high mobility of Re ions would play an important role in the explanation of TPR profiles above discussed.

From H_2 consumption and considering the metal content observed from ICP, we have also calculated the variation in the oxidation state for supported metals (**Table 1**). In the case of monometallic samples, the obtained reduction degrees highlight that after TPR treatment, metal ions were fully reduced from 6+ and 7+ oxidation state for Mo and Re monometallic catalysts respectively.

On the other hand, by observing the reduction degree for the bimetallic systems it is clear that Re1-Mo4/ZSM-5 from Re1st series would show a particular behaviour. For this catalyst, a fraction of the metal content would remain partially oxidized (on average, 67% of ions are reduced). This would clearly imply that the chemical state of Mo has been modified, showing the coexistence of Re-Mo species that are stabilized in a partial oxidized state. Such behaviour is not observed in the similar catalyst from Mo1st series or even for Re4-Mo4 catalysts. Therefore, the order in the sequential incorporation notably condition the final structural and chemical situation of metals.

Table 1. Metal content and H_2 consumption from TPR and oxidation state variation for Re-Mo/ZSM-5 from both series.

	Catalysts	Re wt% *	Mo wt% *	μmol H_2/mg_{cat}	Average reduction %
	Mo4/ZSM-5	---	4.2	1.16	88
	Re1/ZSM-5	1.3	---	0.23	93
	Re4/ZSM-5	3.6	---	0.66	97
Re1st	Re1-Mo4/ZSM-5	0.8	4.2	0.98	67
	Re4-Mo4/ZSM-5	2.3	3.8	1.43	91
Mo1st	Re1-Mo4/ZSM-5	1.2	3.8	1.25	99
	Re4-Mo4/ZSM-5	3.0	3.8	1.36	81

* *Metal content from ICP analysis*.

In **Figure 6** we show the XPS Mo *3d* and Re *4f* spectra for all samples after soft oxidation at 250ºC. The binding energy for Mo $3d_{5/2}$ in Mo4/ZSM-5 is located at 233.3 eV, which has been reported for Mo^{6+} in MoO_3 [25,26]. On the other hand, in the case of Re4/ZSM-5 the observed

binding energy for Re $4f_{7/2}$ level was 46.1 eV, which is in accordance with values associated to Re^{7+} [27]. In the case of bimetallic Re1-Mo4/ZSM-5 catalysts, Mo *3d* and Re *4f* bands show a slight shift toward lower binding energy values. Such small shift would point out a strong interaction with Re. Indeed, as previously discussed above from TPR experiments we have denoted a different reduction profile and a lower reduction degree in the case of Re1st series. Additionally, from BET surface area and acidity measurements we also pointed out such possibility. Thus, when rhenium is present it can be assumed that Mo and Re form a new entity in close interaction.

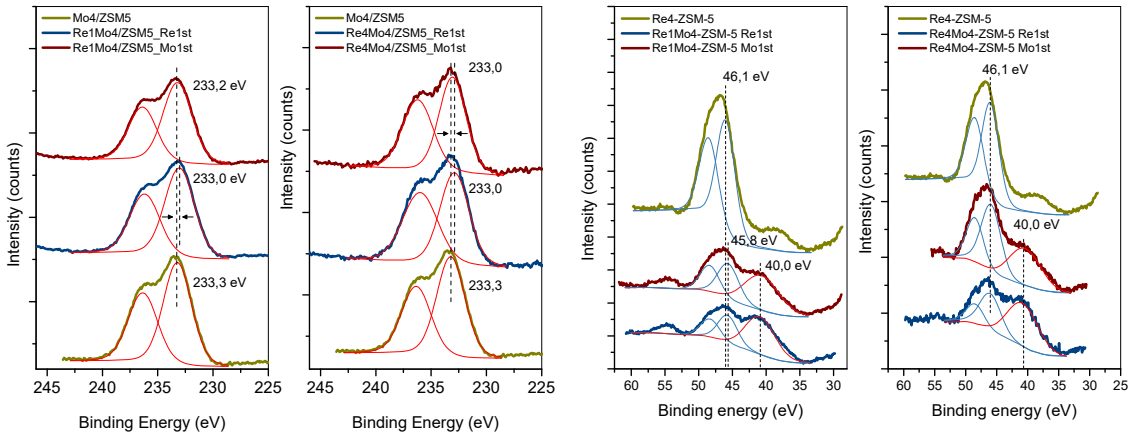

Figure 6. XPS Mo *3d* and Re *4f* core-level spectra for monometallic and bimetallic Mo-Re/ZSM-5 catalysts after soft oxidation at 250 ºC.

If we consider the surface composition (**Table S1**), it can be noticed that in the case of Mo similar Mo/Si ratios have obtained for all catalysts, being in all cases close to Mo content in the monometallic one. However, for rhenium the surface content for Re4-Mo4 in the Re1st series lies markedly below the reference value of monometallic one (0.013 vs 0.007 for Re4/ZSM-5 and R4-Mo4/ZSM-5 Re1st respectively). The observed differences could be related in principle to a

different surface content probably due to a certain loss of Re during second calcination but more importantly to a different distribution of rhenium ions due to the second calcination treatment.

In order to confirm the above behaviour we have studied the evolution of the surface during reduction treatment. The results obtained by an *in situ* XPS study of the reduction process of the monometallic (Mo4/ZSM-5 and Re4/ZSM-5) and bimetallic catalysts from both series are shown below.

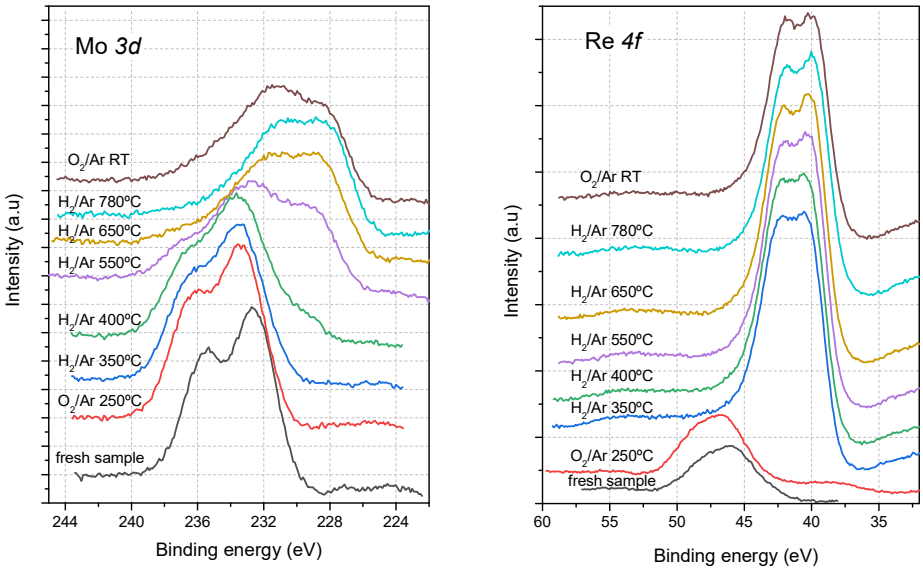

Figure 7. Mo *3d* and Re *4f* regions XPS spectra for the Mo4/ZSM-5 and Re4/ZSM-5 monometallic catalyst calcined and after *in situ* reduction treatment.

The Mo *3d* and Re *4f* regions spectra obtained along different reduction treatments of the monometallic Mo4/ZSM-5 and Re4/ZSM5 systems are shown in **Figure 7**. As previously indicated, for Mo system the only oxidation state present after evacuation pretreatment in O_2 is Mo^{6+} (**Figure 7**). Upon reduction, the Mo *3d* peak doublet becomes less defined pointing out the

co-existence of other species as it was stated from the complex TPR profile. Just after reduction at 650 ºC, the Mo *3d* peak becomes wider and clearly shifted to lower BE (being Mo $3d_{5/2}$ at ca 228.0 eV) denoting that surface Mo is almost reduced to Mo^0 (**Table S1**). Therefore, it can be said that at this temperature all Mo species at the surface got reduced. On the other hand, regarding to Re4/ZSM-5, after calcination the wide peak located at ca 46.1 eV would denote that the main oxidation state is 7+ (**Figure 6**). As observed from TPR, total reduction is achieved at a significantly lower temperature. Indeed after reduction treatment at 350 ºC the Re $4f_{7/2}$ peak at 40 eV clearly points out the complete reduction of Re. It is also worthy to note that the intensity of this peak is notably higher than that for calcined sample. Thus, it is evidenced that upon reduction a notable Re surface enrichment is taking place (**Figure 7**).

The evolution of Re-Mo bimetallic catalysts upon reduction is shown in **Figures 8 and 9**. In the case of molybdenum, Re1-Mo4 and Re4-Mo4 catalysts follow similar reduction evolution within each different series (**Figure 8 and 9**). Mo reduction is taking place in both series at slightly lower temperature with respect to that observed for Mo-monometallic catalyst. Irrespective of the Re amount or addition sequence, contributions of reduced Mo species can be seen at 400 ºC. On the other hand, in the case of Re almost complete reduction is achieved upon treatment at 350 ºC, which agrees with the behaviour observed for monometallic Re catalyst.

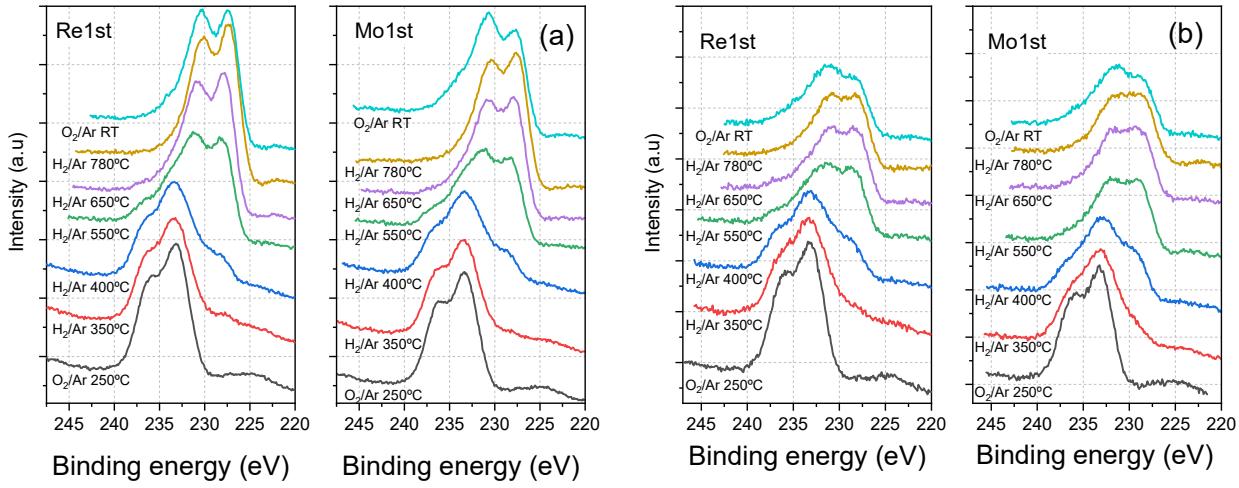

Figure 8. Mo *3d* region XPS spectra for a) Re1-Mo4/ZSM-5 catalysts and b) Re4-Mo4/ZSM-5 catalysts from both series calcined and after in *situ* reduction.

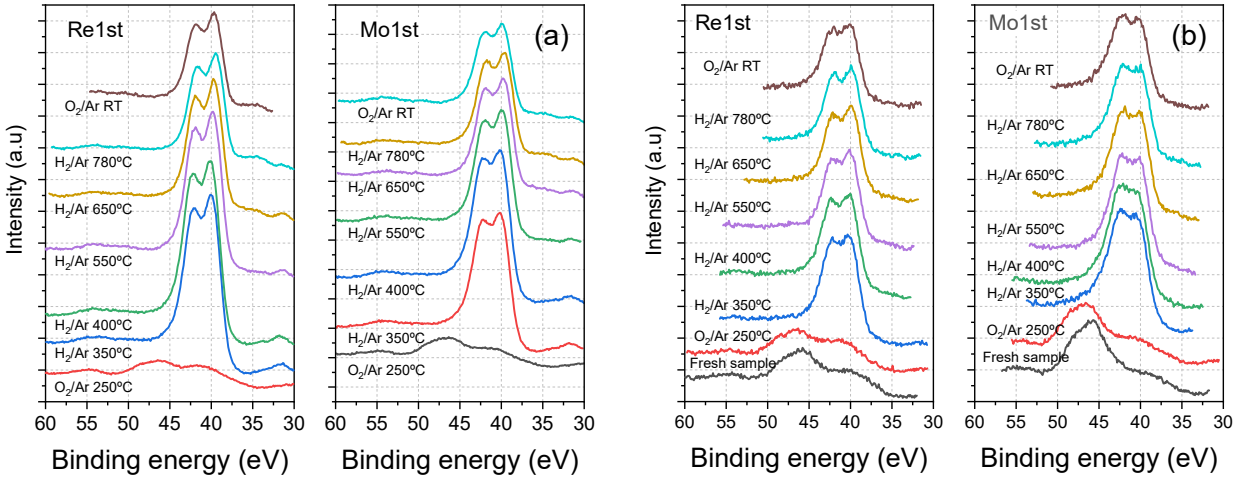

Figure 9. Re *4f* region XPS spectra for a) Re1-Mo4/ZSM-5 catalyst and b) the Re4-Mo4/ZSM-5 catalyst from both series calcined and after in *situ* reduction. (Notice that Mo *2p* peak appears at the same region than Re *4f)*.

As previously pointed out for monometallic systems, an important Re enrichment can be also observed in these bimetallic systems. In **Figure 10** we have plotted the evolution of Re/Si and Mo/Si ratios for all catalyst along the reduction treatment. As a general trend we can state that surface Re/Si ratio seems to increase in the first stage of reduction treatment, after which starts to decay. This would point out that after the first surface enrichment, a slight loss of Re by sublimation or even certain aggregation forming higher size clusters.

On the contrary, for Mo/Si ratio more stable evolution is attained though certain slight decrease can be observable for monometallic catalyst and more markedly for Re4-Mo4 bimetallic catalyst.

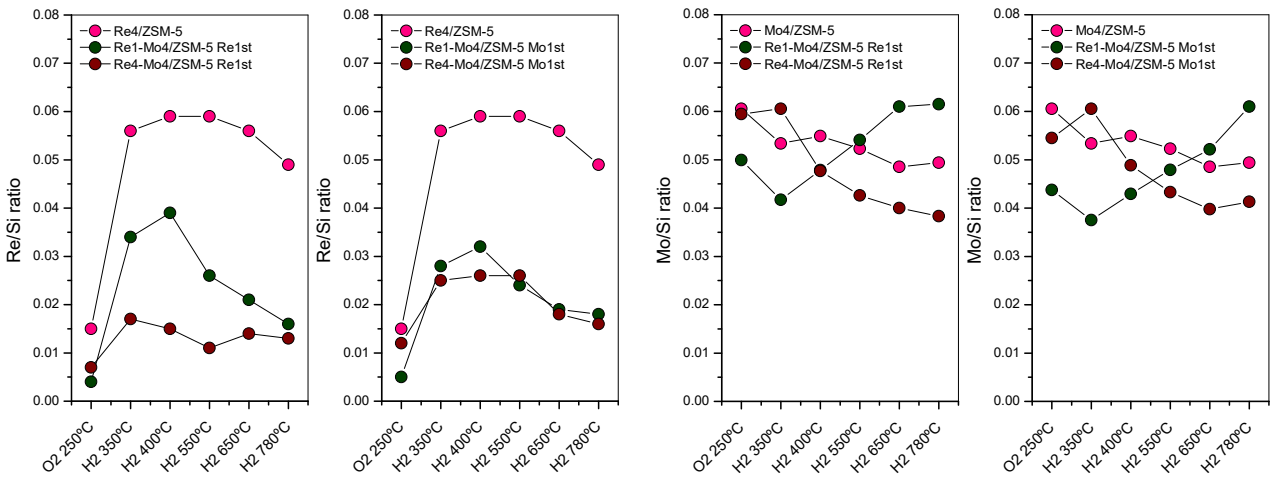

Figure 10. Evolution of the Re/Si and Mo/Si surface ratios upon reduction treatment.

It is worthy to note that for Re1-Mo4 the evolution is the opposite, as Mo/Si surface ratio exhibits a progressive increase. This would indicate that Mo clusters could be dispersed upon reduction in the presence of Re. From these results it is clear that the surface follow a complex evolution during reduction at different temperatures and that the presence of Re would strongly affect to the behaviour of Mo upon reaction conditions denoting the observed strong interaction of both metals.

Thus, Mo would show certain dispersion/enrichment for Re1-Mo4/ZSM-5 while would suffer aggregation as reduction temperature increases for Re4-Mo4. This later aggregation would be associated to the formation of Mo-Re species as was discussed from TPR results. All this particular behaviour could be correlated with the different catalytic behaviour observed for Re-Mo bimetallic catalyst, particularly with low Re content. Within this context, the sequential impregnation would also play an important role, unblocking inner micropores during second calcination and favouring a close Re-Mo interaction that would lead to Re-Mo stabilized against reduction.

CONCLUSIONS.

The incorporation of rhenium as co-dopant to the Mo/ZSM-5 catalyst have showed a notable improvement in the *MDA* reaction. Benzene/aromatics yields for bimetallic systems appeared significantly enhanced. Moreover, the catalytic performance of bimetallic systems is clearly affected by the sequence addition of metals. Thus, best catalytic behaviour has been attained for Re1-Mo4/ZSM-5 in which Re has been firstly deposited (Re1st series).

Due to the high mobility of Re ions, for the Re1st series Re would undergo a particular evolution that conditions the further Mo incorporation. This fact has been stated through the wide surface and structural characterization of the systems. Based on these results, we evidenced that Re ions would be preferentially located at strong acid sites. This fact modifies also the state of Mo species, which showed a close interaction with Re entities. As a result, the C-C coupling step would be favoured which seems to be the responsible of the catalytic performance improvement.

ASSOCIATED CONTENT

Supporting Information. It is available in a separate file.

AUTHOR INFORMATION

Corresponding Author

Email: gcolon@icmse.csic.es

Present Addresses

Instituto de Ciencia de Materiales de Sevilla (CSIC-University of Seville) and Departamento de Química Inorgánica. University of Seville. Av. Américo Vespucio. 49. 41092 Seville. Spain

ACKNOWLEDGMENT

We thank the "Ministerio de Economía and Competitividad" of Spain (Projects ENE2017-88818-C2-1-R and CTQ2014-60524-R). the EU FEDER program and the "Junta de Andalucía" (Projet US-1263455 and FQM015 group) for financial support.

REFERENCES

[1] L. Wang, L. Tao, M. Xie, G. Xu, J. Huang, Y. Xu, Dehydrogenation and Aromatization of Methane under Non-Oxidizing Conditions. Catal. Letters, 21 (1993) pp 35–41.

[2] J.N. Armor, Emerging Importance of Shale Gas to Both the Energy & Chemicals Landscape. J. Energy Chem., 22 (2013) pp 21–26.

[3] D. Kiani, S. Sourav, Y. Tang, J. Baltrusaitis, I.E. Wachs, Methane activation by ZSM-5-supported transition metal centers. Chem. Soc. Rev. 50 (2021) pp 1251–1268.

[4] N. Kosinov, E.A. Uslamin, F.J.A. Coumans, A.S.G. Wijpkema, R.Y. Rohling, E.J.M. Hensen Structure and evolution of confined carbon species during methane dehydroaromatization over Mo/ZSM-5. ACS Catal. 8 (2018) pp 8459–84677.

[5] S.J. Han, S.K. Kim, A. Hwang, S. Kim, D.Y. Hong, G. Kwak, K.W. Jun, Y.T. Kim, Non-Oxidative dehydroaromatization of methane over Mo/H-ZSM-5 catalysts: A detailed analysis of the reaction-regeneration cycle. Appl. Catal. B Environ. 241 (2019) pp 305–318.

[6] Tempelman, C. H. L.; Hensen, E. J. M. On the Deactivation of Mo/HZSM-5 in the Methane Dehydroaromatization Reaction. Appl. Catal. B Environ. 176–177 (2015) pp 731–739.

[7] Y. Gu, P. Chen, H. Yan, X. Wang, Y. Lyu, Y. Tian, W. Liu, Z. Yan, X. Liu, Coking mechanism of Mo/ZSM-5 catalyst in methane dehydroaromatization. Appl. Catal. A: Gen. 6135 (2021) 118019.

[8] U. Menon, M. Rahman, S.J. Khatib. A critical literature review of the advances in methane dehydroaromatization over multifunctional metal-promoted zeolite catalysts. Appl. Catal. A: Gen. 608 (2020) 117870.

[9] Tshabalala, T. E.; Coville, N. J.; Scurrell, M. S. Dehydroaromatization of methane over doped Pt/Mo/H-ZSM-5 zeolite catalysts : The Promotional Effect of Tin. Appl. Catal. A, Gen. 485 (2014) pp 238–244.

[10] V. Abdelsayed, D. Shekhawat, M.W. Smith, Effect of Fe and Zn Promoters on Mo/HZSM-5 Catalyst for Methane Dehydroaromatization. Fuel 139 (2015) pp 401–410.

[11] Y. Zhang, M. Kidder, R.E. Ruther, J. Nanda, G.S. Foo, Z. Wu, C.K. Narula, Promotional effects of In on non-oxidative methane transformation over Mo-ZSM-5. Catal. Letters 146 (2016) pp 1903–1909.

[12] A. Sridhar, M. Rahman, A. Infantes-Molina, B.J. Wylie, C.G. Borcik, S.J. Khatib. Bimetallic Mo-Co/ZSM-5 and Mo-Ni/ZSM-5 Catalysts for Methane Dehydroaromatization: A Study of the Effect of Pretreatment and Metal Loadings on the Catalytic Behaviour. Appl. Catal. A Gen. 589 (2020) 117247.
[13] P. Schwach, X. Pan, X. Bao. Direct Conversion of Methane to Value-Added Chemicals over Heterogeneous Catalysts: Challenges and Prospects. Chem. Rev. 117 (2017) pp 8497–8520.
[14] A.M. Hilmen, D. Schanke, A. Holmen, TPR study of the mechanism of Rhenium promotion of alumina-supported Cobalt Fischer-Tropsch catalysts. Catal. Letters 38 (1996) pp 143–147.
[15] I. Vollmer, E. Abou-Hamad, J. Gascón, F. Kapteijn, Aromatization of Ethylene – Main Intermediate for MDA? ChemCatChem, 12 (2020) pp 544–549.
[16] A. Galadima, O. Muraza. Advances in Catalyst design for the conversion of methane to aromatics: A critical review. Catal. Surv. Asia 23 (2019) pp 149–170.
[17] N. K. Razdan, A. Kumar, B. L. Foley, A. Bhan. Influence of ethylene and acetylene on the rate and reversibility of methane dehydroaromatization on Mo/H-ZSM-5 catalysts. J. Catal. 381 (2020) pp 261–270.
[18] N. Kosinov, F.J.A.G. Coumans, G. Li, E. Uslamin, B. Mezari, A.S.G. Wijpkema, E.A. Pidko, E.J.M. Hensen. Stable Mo/HZSM-5 methane dehydroaromatization catalysts optimized for stable Mo/HZSM-5 methane dehydroaromatization catalysts optimized for high-temperature calcination-regeneration. J. Catal. 346 (2017) pp 125–133.
[19] H.S. Lacheen, P.J. Cordeiro, E. Iglesia, Structure and catalytic function of Re-oxo species grafted onto H-MFI zeolite by sublimation of Re_2O_7. J. Am. Chem. Soc. 128 (2006) pp 15082-15083
[20] W. Gao, G. Qi, Q. Wang, W. Wang, S. Li, I. Hung, Z. Gan, J. Xu, F. Deng. Dual active sites on Molybdenum/ZSM-5 catalyst for methane dehydroaromatization: Insights from solid-state NMR spectroscopy. Angew. Chem. Int. Ed. 60 (2021) pp 10709–10715.
[21] Wang, A.; He, P.; Yung, M.; Zeng, H.; Qian, H.; Song, H. Catalytic Co-Aromatization of Ethanol and Methane. Appl. Catal. B Environ. 2016, 198, 480–492.
[22] A. López-Martín, A. Caballero, G. Colón. Structural and surface considerations on Mo/ZSM-5 systems for methane dehydroaromatization reaction. Mol. Catal. 486 (2020) pp 110787.

[23] A. López-Martín, F. Platero, G. Colón, A. Caballero. Elucidating the nature of Mo species on ZSM-5 and its role in the methane aromatization reaction. React. Chem. Eng. 6 (2021) pp 1265–1276.

[24] T. Otsuka, N. Sawano, Y. Fujii, T. Omura, C. Taylor, M. Shimada. Effects of rhenium contents on oxidation behaviours of tungsten-rhenium alloys in the oxygen gas atmosphere at 873 K. Nucl. Mater. Energy 25 (2020) 1007913.

[25] J.-G. Choi, L.T. Thompson. XPS study of as-prepared and reduced molybdenum oxides. Appl. Surf. Sci. 93 (1996) pp 143–149.

[26] T. Schroeder, J. Zegenhagen, N. Magg, B. Immaraporn. H.-J. Freund. Formation of a faceted MoO_2 epilayer on Mo(1 1 2) studied by XPS, UPS and STM. Surf. Sci. 552 (2004) pp 85–97.

[27] V.V. Kuznetsov, Y.D. Gamburg, V.V. Zhulikov, R.S. Batalov, E.A. Filatova. Re-Ni cathodes obtained by electrodeposition as a promising electrode material for hydrogen evolution reaction in alkaline solutions. Electrochim. Acta 317 (2019) pp 358–366.